Appl. Phys. B (2013) 113:339–344
DOI 10.1007/s00340-013-5495-1

Applied Physics B
Lasers and Optics

Generation of THz transients by photoexcited single-crystal GaAs meso-structures

Jie Zhang · Martin Mikulics · Roman Adam · Detlev Grützmacher · Roman Sobolewski

Published online: 25 May 2013

Abstract We report a sub-picosecond photoresponse and THz transient generation of GaAs single-crystal mesoscopic platelets excited by femtosecond optical pulses. Our structures were fabricated by a top-down technique, by patterning an epitaxial, 500-nm-thick GaAs film grown on top of an AlAs sacrificial layer and then transferring the resulting etched away $10 \times 20\text{-}\mu m^2$ platelets onto an MgO substrate using a micropipette. The freestanding GaAs devices, incorporated into an Au coplanar strip line, exhibited extremely low dark currents and ~ 0.4 % detection efficiency at 10 V bias. The all-optical, pump–probe carrier dynamics analysis showed that, for 800-nm-wavelength excitation, the intrinsic relaxation of photocarriers featured a 310-fs-wide transient with a 290 fs fall time. We have also carried out a femtosecond, time-resolved electro-optic characterization of our devices and recorded along the transmission line the electrical transients as short as ~ 600 fs, when the platelet was excited by a train of 100-fs-wide, 800-nm-wavelength optical laser pulses. The platelets have been also demonstrated to be very efficient generators of free-space propagating THz transients with the spectral bandwidth exceeding 2 THz. The presented performance of the epitaxial, freestanding GaAs meso-structured photodevices makes them uniquely suitable for THz-frequency optoelectronic applications, ranging from ultrafast photodetectors to THz-bandwidth optical-to-electrical transducers and photomixers.

J. Zhang · R. Sobolewski
Department of Electrical and Computer Engineering and Laboratory for Laser Energetics, University of Rochester, Rochester, NY 14627-0231, USA

Present Address:
J. Zhang
Center for Visual Science, University of Rochester, Rochester, NY 14642, USA

M. Mikulics · D. Grützmacher
Peter Grünberg Institut (PGI-9), Research Centre Jülich, Jülich 52425, Germany

M. Mikulics · R. Adam · D. Grützmacher
Jülich-Aachen Research Alliance (JARA)-Fundamentals of Future Information Technology, 52425 Jülich, Germany

R. Adam
Peter Grünberg Institut (PGI-6), Research Centre Jülich, Jülich 52425, Germany

R. Sobolewski (✉)
Department of Physics and Astronomy and the Materials Science Program, University of Rochester, Rochester, NY 14627, USA
e-mail: roman.sobolewski@rochester.edu

R. Sobolewski
Institute of Electron Technology, 02668 Warszawa, Poland

1 Introduction

Terahertz (THz) radiation, commonly understood to correspond to frequencies from approximately 0.1 to 30 THz, has very desired properties for a wide range of applications, such as non-destructive evaluation and inspection, biology and medical sciences, spectroscopic studies of carrier and intermolecular dynamics, short-range information transfer and communications, and homeland security [1–3]. The generation of transient THz signals (THz bursts) can be achieved by a variety of techniques, including ultrafast switching of photoconductive antennas and optical rectification in nonlinear crystals [3]. Technological innovation in photonics and nanoscience enable novel THz generation techniques, such as coherent excitation of acoustic waves or polar optical phonons, laser induced gas plasma, and carrier

tunneling in coupled double-quantum-well structures [4–7]. However, optically excited photoconductive antennas are still the most efficient devices for THz radiation generation, reliably providing high-intensity and wide-spectral bandwidth signals. Such antennas are widely applied in THz time-domain spectroscopy, with GaAs crystals used as photoconductive emitters, due to their excellent electronic transport and optoelectronic properties. Independently, during the last decade, there has been an explosive growth of interest in novel devices, based on nanometer-sized structures [8, 9]. Most recently, we have demonstrated THz response from a single-crystal GaAs meso-whisker, as well as presented its ultra-high-speed photodetector operation with a repetition rate of above 1 THz [10].

In this communication, we will report our time-resolved characterization of epitaxially grown, single-crystal, freestanding GaAs platelet mesoscopic structures operated as both THz-bandwidth photodetectors and THz transient generators. The next section is devoted to our top-down fabrication process of freestanding GaAs platelets, including our unique transferring method on to a predetermined position on a substrate of choice. Section 3 presents our electrical, all-optical, and time-resolved electro-optic characterization of platelet devices operated as both photodetectors and THz transient generators. Finally, Sect. 4 contains our conclusions.

2 Fabrication of freestanding GaAs mesoscopic platelets

Our freestanding GaAs platelets were fabricated following a so-called Jülich fabrication process [11, 12] that starts with a MBE growth of a planar GaAs back layer on a semi-insulating GaAs substrate, followed by a 50-nm-thick AlAs sacrificial interlayer and, finally, completed with the top, 500-nm-thick GaAs layer. For our devices, the growth process has been performed at 600 °C, in order to obtain GaAs of the highest quality. After the MBE growth, an array of 10×20-μm^2 platelet structures was patterned employing optical lithography and argon ion beam etching. Next, the patterned structure was detached from its native substrate by dissolving the AlAs layer in a HF:H_2O solution and, subsequently, placed on a single-crystal MgO substrate with a help of a special micropipette. The entire patterning, transfer, and positioning procedure is schematically shown in Fig. 1. Using a pipette, we have achieved an overall, 5–10-μm accuracy of the platelet positioning. The bond of our GaAs meso-structure to the MgO substrate was strong enough to enable the subsequent, standard photolithography processing and deposition of a 20-μm-wide Au coplanar strip (CPS) transmission line (10-μm line separation) on top of the ends of the platelet (see Fig. 1 and inset in Fig. 3). To improve morphology and crystallinity of the GaAs platelets and to eliminate possible defects on their sidewalls, the entire structure was annealed for 20 min at 600 °C in nitrogen atmosphere, following Krotkus et al. [13]. During the annealing, the platelet structures were covered with a dummy GaAs substrate to suppress As reduction.

3 Experimental characterization of GaAs platelet photodetectors

3.1 DC measurements

Electrical characterization of our CPS-imbedded platelet photodetector structure was carried out by measuring the current–voltage (*I–V*) characteristics both in the dark and under continuous-wave, 800-nm-wavelength light illumination, with the nominal power of 0.15 mW. For the *I–V* measurement, an HP 8,904 multifunction synthesizer was used as the voltage source and an HP 34401 multimeter was responsible for current readout. The corresponding *I–V* curves are shown in Fig. 2, and we note that they exhibit Ohmic behavior in the tested range of bias voltages. The dark current values were 3.3×10^{-9} A at 10 V. The inset in Fig. 2 shows responsivity of our device as a function of the bias voltage, calculated for the light power actually delivered to the device and estimated to be ~90 μW, and normalized to the platelet optically active area 10×10 μm^2 (see inset in Fig. 3). The device responsivity reaches 2.5 mA/W at the 10-V bias, which corresponds to quite impressive ~0.4 % single-photon detection efficiency.

3.2 All-optical pump–probe studies

To further investigate the intrinsic material photoresponse, we performed all-optical femtosecond pump–probe

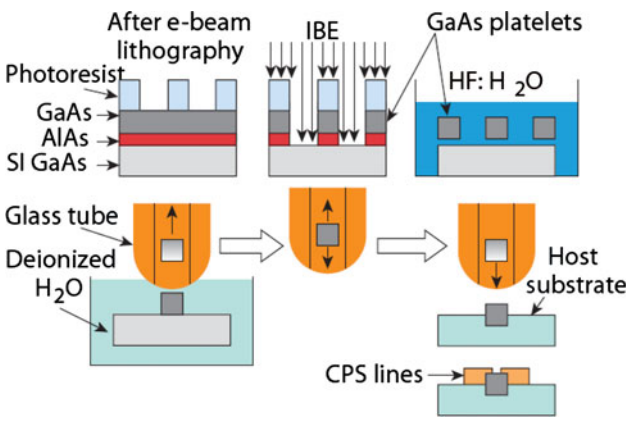

Fig. 1 Schematics of the epitaxial GaAs platelets fabrication process

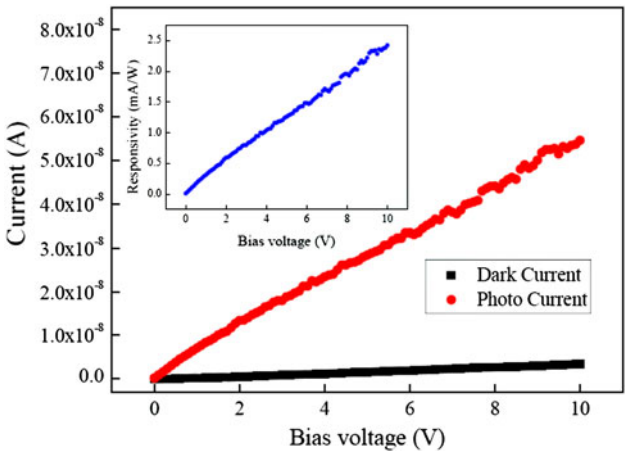

Fig. 2 Current–voltage characteristics of a GaAs freestanding platelet placed on an MgO substrate and incorporated into a CPS transmission line. The characteristics were measured in the *dark* (*black squares*) and under 800-nm-wavelength, 90-μW nominal power continuous illumination (*red circles*), respectively. The *top inset* presents the responsivity of our device

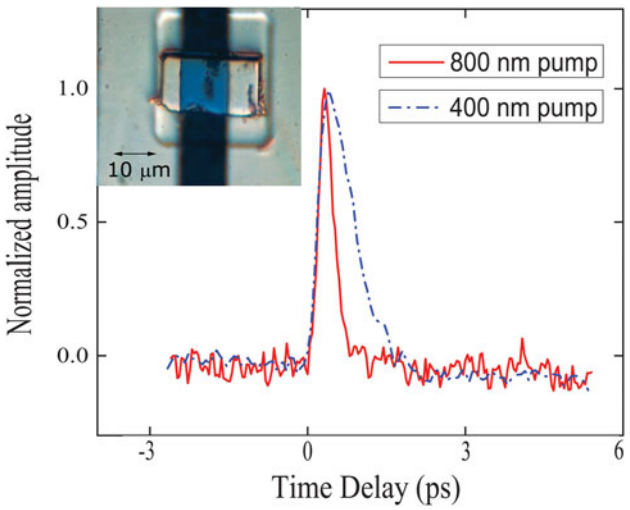

Fig. 3 Pump–probe spectroscopy results of the GaAs platelet with 400-nm (*dot-dashed line*) and 800-nm (*solid line*) illumination. The probe wavelength was 800 nm for both measurements. The inset presents image of the GaAs platelet embedded in a CPS line

spectroscopy studies on the GaAs platelet. Both one-color and two-color pump–probe spectroscopy experiments were performed in reflection mode, using our MIRA oscillator, as well as a second-harmonic generator. The output from MIRA features a 100-fs-wide, linearly polarized, Gaussian pulse train with the wavelength centered at 800 nm. In the two-color version, the second-harmonic 400-nm-wavelength pulses with the width of ~150 fs were used as the pump and focused on the sample surface with a spot diameter of ~20 μm and the fluence of ~0.04 mJ/cm^2 per pulse. The 800-nm-wavelength probe pulses were aimed perpendicular to the sample surface with a diameter of ~10 μm, and their fluence was much smaller (at least in the factor of 10) than that of the pump. The smaller spot size of the probe ensured that we probed a region with uniform photoexcitation. For the signal detection, the probe reflection from the sample surface was filtered by a NIR-pass filter and collected by a photodetector, whose signal was measured by a lock-in amplifier, synchronized with an acousto-optic modulator operating at a frequency of 99.8 kHz. Figure 3 shows both the one-color (800-nm/800-nm) and two-color (400-nm/800-nm) optical pump–probe time-resolved photoresponse normalized reflectivity change $\Delta R/R$ transients, denoted as the solid and dot-dashed lines, respectively. For 800-nm excitation, the $\Delta R/R$ signal has a full-width-at-half-maximum (FWHM) of 310 fs and fall time of 290 fs, which agrees very well with our characterization of the intrinsic photoresponse of a freestanding whisker meso-structure [10]. The latter indicates that the demonstrated THz-bandwidth optoelectronic performance of our both whisker- and platelet-type devices is the material, rather than geometry limited.

For 400-nm-wavelength excitation, the $\Delta R/R$ transient presented in Fig. 3 is significantly longer than that for 800-nm excitation. The pulse in this case has ~780 fs FWHM and ~1 ps decay time. This significant broadening effect can be explained by two main factors. First, for blue light, due to its very small, ~100 nm, optical penetration depth into GaAs, highly excited carriers are generated mostly at the surface, and at the early relaxation phase, they will efficiently relax via emission of optic phonons. Thus, near the surface, we have very high excess concentrations of carriers and phonons, leading to the enhanced, both carrier–carrier and carrier–phonon scattering, and resulting a suppressed mobility μ [14]. The 1-to-5 ratio between the 400-nm light optical penetration and the sample 500 nm thickness also means that the photogenerated carriers near the surface require an additional time for diffusion through the sample volume. Second, since the initial excess energy of photocarriers is ~1.6 eV, they are very likely to efficiently scatter into the satellite L and X valleys, as their minima in GaAs are only 0.29 and 0.48 eV above the Γ valley minimum, respectively. The intervalley scattering occurs on the 10–100 fs time scale, via emission of large wave-vector phonons [15], and these phonons must decay through a multi-phonon process. The observed, approximately 1-ps-wide $\Delta R/R$ transient for the 400-nm/800-nm pump–probe configuration agrees well with the above arguments.

We need to stress that under 800-nm-wavelength illumination, the FWHM of the $\Delta R/R$ photoresponse is 310 fs, which is essentially identical to the FWHM reported for the low-temperature-grown (LT-GaAs) material [16], widely

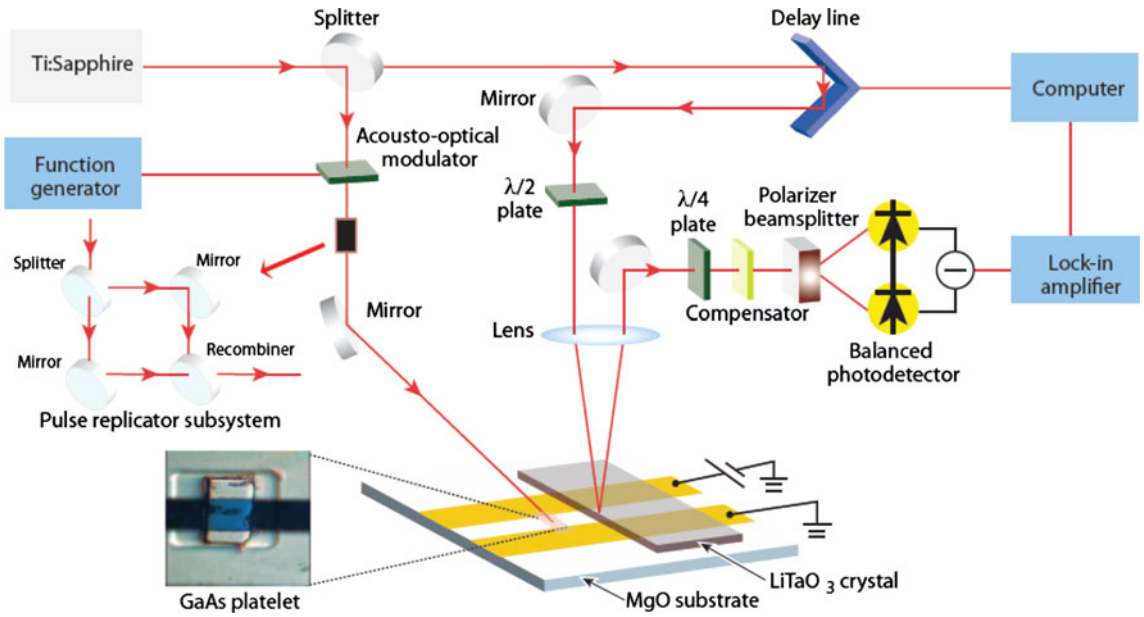

Fig. 4 Schematic configuration of our sub-picosecond, time-domain, EOS measurements. The signal, generated by the GaAs platelet mesostructure upon laser double-pulse excitation is coupled to the CPS transmission line and detected by means of the Pockels effect via a $LiTaO_3$ crystal (light rectangle overlaying the CPS). The linearly polarized sampling beam is set at 45 with respect to the EO crystal's optical axis. The two insets on the *left-hand corner* show our pulse replicator subsystem for double-pulse excitation experiments and a micrograph of our actual GaAs platelet device imbedded into a CPS line

used for ultrafast optoelectronic devices. It is well known that in LT-GaAs, structure defects, and As precipitates are responsible for carrier trapping—the key mechanism responsible for the LT-GaAs ultrafast response. Our devices, however, have been made of high-quality, single-crystal GaAs with μ as high as $\sim$7,300 cm^2/V s [10]. More research in this aspect is clearly needed, including, possibly, extensive Monte Carlo simulations of the carrier transport in GaAs with the various levels of carrier trapping.

3.3 Electro-optic time-resolved photodetector studies

To further confirm the intrinsic nature of the sub-picosecond (THz-bandwidth) carrier relaxation dynamics in our freestanding GaAs devices, we have performed a series of electro-optic sampling (EOS) experiments on the GaAs platelet. As in the case of a GaAs whisker photodetector [10], the photoresponse electrical transients were measured using a $LiTaO_3$ crystal with a bottom high-reflectivity coating acting as an ultrafast EO transducer. Detailed schematics of our EOS experimental setup is shown in Fig. 4. Electrical transients were generated by exciting the platelet with a pair of 100 fs in duration, 800-nm-wavelength laser pluses generated by a Ti: sapphire laser. Their separation externally controlled and varied from one to a few picoseconds with the help of a homemade pulse replicator (see inset in Fig. 4). Next, the photoexcited electrical transients were coupled via the 45-Ω characteristic impedance CPS into the EO transducer and—by means of the Pockels effect—converted into the polarization-state change of optical sampling pulses incident on $LiTaO_3$ and time-correlated with the excitation pulses. The sampling beam traveled through a computer-controlled delay line, polarizer, and a microscope objective. The sampling beam was 45° linearly polarized with respect to the optical axis of the $LiTaO_3$ EO sensing crystal, and, after reflection from the high-reflectivity coating at the crystal bottom, it was guided to the compensator, the analyzer, and, finally, a pair of 125-MHz bandwidth low-noise, differential photoreceivers.

An example of the experimental electrical photoresponse transient is shown in Fig. 5, when the excitation pulses were separated by 1.1 ps. We can see two well-separated voltage pulses, each having the 680 fs FWHM. The magnitude of the photoresponse reaches almost zero between the two pulses, which must mean that not only the platelet photodetector exhibits a sub-picosecond (THz-bandwidth) transient response, but also our photoexcited carriers excited by the first pulse managed to almost reach their equilibrium state before the arrival of the second one. The inset in Fig. 5 presents the fastest, 600-fs-wide voltage transient, when the sampling point located at the edge of the $LiTaO_3$ sensing crystal (see Fig. 4) was only $\sim$110 μm away from the platelet. The latter EO measurement was performed using a single optical pulse excitation. We stress

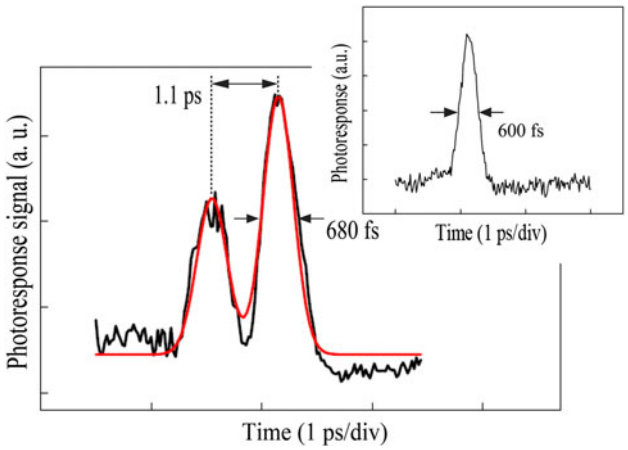

Fig. 5 Transient photoresponse of a GaAs platelet photodetector illuminated with a train of two 100-fs-wide, 800-nm-wavelength, and 1-mW incident power optical pulses. The detector bias was 20 V. The *black line* is an experimental signal recorded at ~150 μm away from the device plane (see Fig. 4), while the *red line* is a numerical fit representing a combination of the error functions (rise portions of the pulses) and the single-exponential decay (relaxation parts). The difference in the amplitudes of the first and the second photoresponse pulses is due to an approx. 40/60 beam splitter used in the pulse replicator subsystem (see Fig. 4). The inset presents a 600-fs-wide voltage transient obtained using a single optical pulse excitation and recorded when a sampling point was ~110 μm away from the platelet plane

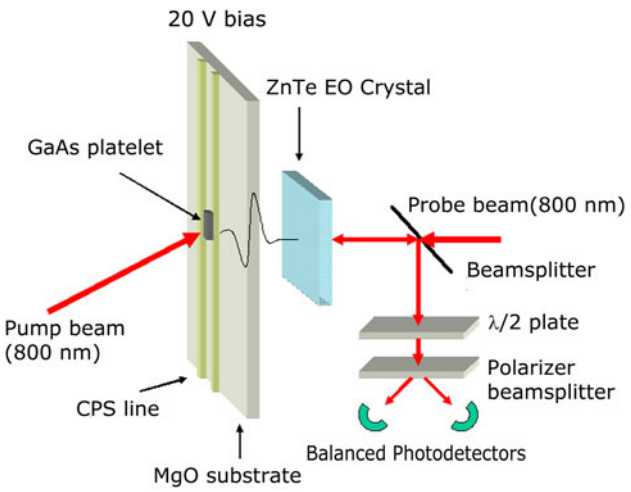

Fig. 6 Schematics of a transient THz measurement apparatus. The signal, generated by a voltage-biased (20 V) GaAs platelet meso-structure upon laser excitation, propagates through the back of the MgO substrate and is detected by means of the Pockels effect via a ZnTe crystal with a high reflectivity back side. The sampling beam polarization change detection setup is analogous to that presented in Fig. 4

that the two-pulse experiment directly demonstrates that our meso-structured devices can operate successfully even when they are exposed to optical input trains (e.g., optical clock signals) with the THz repetition rate.

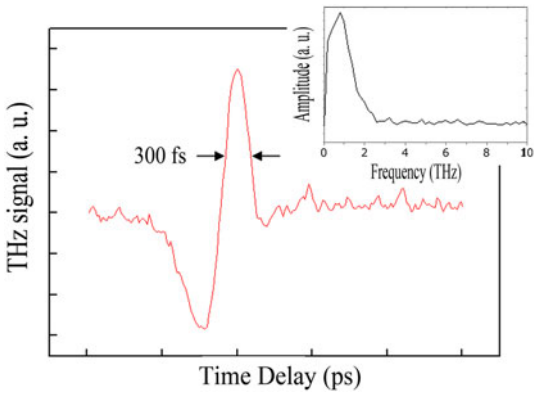

Fig. 7 Free-space THz transient generated by a freestanding GaAs platelet photoexcited by a 100-fs-wide, 800-nm-wavelength optical pulse and biased at 20 V. The inset shows the Fourier transform of the signal, with a center frequency of ~1.3 THz

3.4 Free-space THz transient generation

Finally, we have performed a free-space, THz time-domain spectroscopy on the freestanding GaAs platelet. Our experimental setup for THz transient generation is shown in Fig. 6. Again, 800-nm-wavelength, 100-fs-wide pulses from our Ti: sapphire laser were used, and the device was biased at 20 V applied to the CPS. Following Ref. [17], a 2-mm-thick ZnTe single crystal, acting as an EO THz sensor, was put ~1 mm behind the sample for the free-space THz detection. Figure 7 presents the time-resolved, single-oscillation-type THz pulse generated by our GaAs sample and detected along the main axis of the signal propagation. The inset in Fig. 7 shows the fast Fourier transform of the experimental transient and the center frequency is at the 1.3 THz point.

4 Conclusion

We have presented DC characteristics, all-optical pump–probe spectroscopy, in-plane time-domain EO sampling, and free-space THz spectroscopy results of freestanding, epitaxially grown GaAs platelets fabricated via a top-down photolithography method, transferred onto a crystalline MgO substrate and incorporated into a CPS transmission line structure. As a photodetector, our freestanding, epitaxial GaAs element is truly unique, since it combines extremely low dark currents and the responsivity as high as 2.5 mA/W with a sub-picosecond photoresponse, and assures successful operation even in optical systems with THz laser clock-pulse rates. The platelet structure has also been demonstrated to be a very efficient generator of free-space propagating THz transients with the bandwidth extending beyond 2 THz.

Acknowledgments The authors thank P. Song and M. Samuels for their assistance in early experiments. This work is supported in part by ARO Grant No. W911NF-12-2-0076 (Rochester). J. Z. acknowledges support from the Frank Horton Graduate Fellowship Program at the University of Rochester Laboratory for Laser Energetics, funded by the US Department of Energy Office of Inertial Confinement Fusion under Cooperative Agreement No. DE-FC52-08NA28302 and the New York State Energy Research and Development Authority. The support of ARO and DOE does not constitute their endorsement of the views expressed in this article.

References

1. A. Redo-Sanchez, X.-C. Zhang, Terahertz science and technology trends. IEEE J. Sel. Top. Quantum Electron. **14**(2), 260–269 (2008)
2. P.H. Siegel, Terahertz technology in biology and medicine. IEEE Trans. Microw. Theory Tech. **52**(10), 2438–2447 (2004)
3. C.A. Schmuttenmaer, Exploring dynamics in the far-infrared with terahertz spectroscopy. Chem. Rev. **104**, 1759–1779 (2004)
4. S. Wu, J. Zhang, A. Belousov, J. Karpinski, R. Sobolewski, Ultralong-lived coherent acoustic phonons in GaN single crystals. J. Phys: Conf. Ser. **92**, 012021 (2007)
5. M.R. Armstrong et al., Observation of terahertz radiation coherently generated by acoustic waves. Nat. Phys. **5**, 285–288 (2009)
6. J. Dai, J. Liu, X.-C. Zhang, Terahertz wave air photonics: terahertz wave generation and detection with laser-induced gas plasma. IEEE J. Sel. Top. Quantum Electron. **17**, 183–190 (2011)
7. H.G. Roskos et al., Coherent submillimeter-wave emission from charge oscillations in a double-well potential. Phys. Rev. Lett. **68**(14), 2216–2219 (1994)
8. K. Hiruma et al., Growth and optical properties of nanometer-scale GaAs and InAs whiskers. J. Appl. Phys. **77**, 447 (1995)
9. Y. Cui et al., Nanowire nanosensors for highly sensitive and selective detection of biological and chemical species. Science **293**, 1289 (2001)
10. M. Mikulics et al., Subpicosecond electron-hole recombination time and terahertz-bandwidth photoresponse in freestanding GaAs epitaxial mesoscopic structures. Appl. Phys. Lett. **101**, 031111 (2012)
11. R. Adam et al., Fabrication and subpicosecond optical response of low-temperature-grown GaAs freestanding photoconductive devices. Appl. Phys. Lett. **81**, 3485 (2002)
12. M. Mikulics et al., High-speed photoconductive switch based on low-temperature GaAs transferred on SiO_2/Si substrate. IEEE Photonics Technol. Lett. **15**, 528 (2003)
13. A. Krotkus et al., Picosecond carrier lifetime in GaAs implanted with high doses of as ions: an alternative to low-temperature GaAs for optoelectronic applications. Appl. Phys. Lett. **66**, 3304 (1995)
14. M.C. Beard, G.M. Turner, C.A. Schmuttenmaer, Transient photoconductivity in GaAs as measured by time-resolved THz spectroscopy. Phys. Rev. B. **62**, 15764–15777 (2000)
15. A. Othonos, Probing ultrafast carrier and phonon dynamics in semiconductors. J. Appl. Phys. **83**, 1789 (1998)
16. X. Zheng et al., Femtosecond photoresponse of a Freestanding LT-GaAs photoconductive switch. Appl. Opt. **42**, 1726 (2003)
17. Q. Wu, M. Litz, X.-C. Zhang, Broadband detection capability of ZnTe electro-optic field detectors. Appl. Phys. Lett. **68**(21), 2924 (1996)